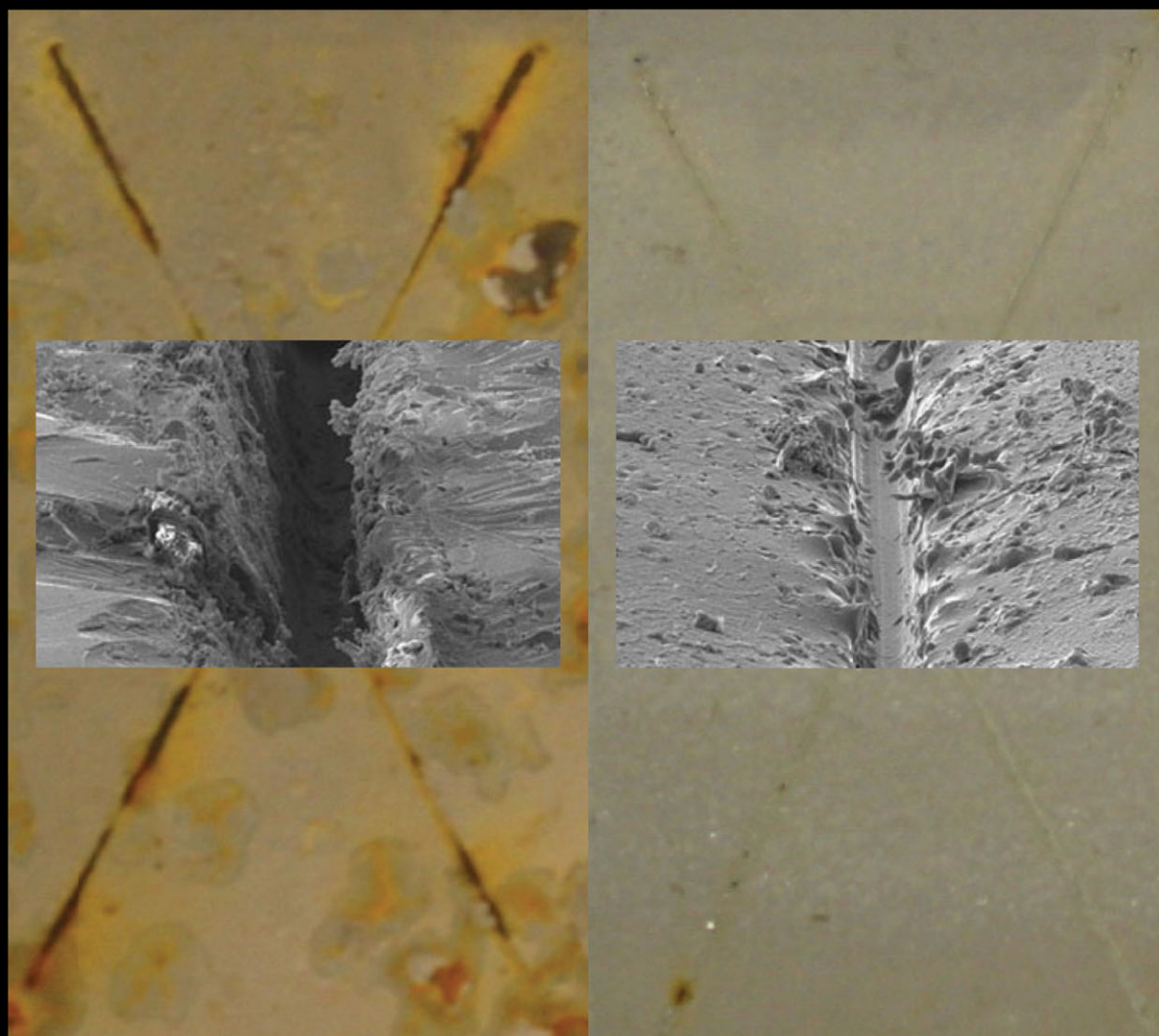


ADVANCED MATERIALS



SELF-HEALING POLYMERS

These images present the dramatic reduction in corrosion of a steel plate coated with a self-healing coating (right) as compared to a conventional coating. Both samples were scratched and placed in 5% NaCl for 5 days. The background is an optical image (2x magnification), in the foreground is an SEM image of the scratch. In the self-healing sample, the scratch has almost completely self-healed, while in the control sample, the scratch remains all the way down to the substrate, as reported by Paul Braun and co-workers on p.645.

Self-Healing Polymer Coatings

By Soo Hyoun Cho, Scott R. White, and Paul V. Braun*

Autonomic healing materials respond without external intervention to environmental stimuli in a nonlinear and productive fashion, and have great potential for advanced engineering systems.^[1–21] Self-healing coatings, which autonomically repair and prevent corrosion of the underlying substrate, are of particular interest. Notably, the worldwide cost of corrosion has been estimated to be nearly \$300 billion per year.^[22] Recent studies on self-healing polymers have demonstrated repair of bulk mechanical damage^[1–21] as well as dramatic increases in the fatigue life.^[23,24] Various approaches for achieving healing functionality have been demonstrated, including encapsulation,^[1–7] reversible chemistry,^[8–11] microvascular networks,^[12] nanoparticle phase separation,^[13–15] polyionomers,^[16–18] hollow fibres,^[19,20] and monomer phase separation.^[21] The majority of these systems, however, have serious chemical and mechanical limitations, preventing their use as coatings. Modern engineered coatings are highly optimized materials in which dramatic modifications of the coating chemistry are unlikely to be acceptable. Here, we describe a generalized approach to self-healing polymer-coating systems, and demonstrate its effectiveness for both model and industrially important coating systems.

Polymeric coatings protect a substrate from environmental exposure, and when they fail corrosion of the substrate is greatly accelerated. Because they are typically thin and in direct contact with the environment, some degree of environmental contamination, by for example, O₂ and H₂O, is unavoidable. Thus, in contrast to bulk (thick) self-healing systems, where environmental contaminants can largely be avoided, a self-healing coating must be highly stable to species present in the environment. We previously demonstrated, in a bulk system, a self-healing chemistry based on the di-*n*-butyltin dilaurate catalyzed polycondensation of hydroxyl end-functionalized polydimethylsilox-

ane (HOPDMS) and polydiethoxysiloxane (PDES), which meets this important requirement.^[21] This healing chemistry is attractive because it is air and water stable, and remains active even after exposure to elevated temperatures (up to 150 °C), enabling its use in systems requiring a thermal cure. While the mechanical properties of the resultant cross-linked siloxane are not exceptional, in a coating system the mechanical strength of the healed matrix is of secondary importance, compared to chemical stability and passivating ability, two areas where siloxanes show exceptional performance. We explored two self-healing coating approaches, starting from this siloxane-based materials system. In the first, as presented in Figure 1, the catalyst is microencapsulated, and the siloxanes are present as phase-separated droplets. In the second approach, the siloxanes were also encapsulated and dispersed in the coating matrix. Encapsulation of both phases (the catalyst and the healing agent) is advantageous in cases where the matrix can react with the healing agent.

Our initial model system consists of an epoxy vinyl ester matrix, 12 wt% phase-separated healing agent, 3 wt% polyurethane (PU)-microencapsulated dimethyldi-n-decanoate tin (DMDNT) catalyst solution, and 3 wt% methylacryloxy propyl triethoxy silane adhesion promoter. The percentages of each component are selected based on our prior experiments on self-healing of bulk materials.^[21] The PDMS-based healing agent is a mixture of 96 vol% HOPDMS and 4 vol% PDES, and the catalyst solution consists of 5 wt% DMDNT in chlorobenzene. The DMDNT/chlorobenzene-filled PU capsules average 90 μm in

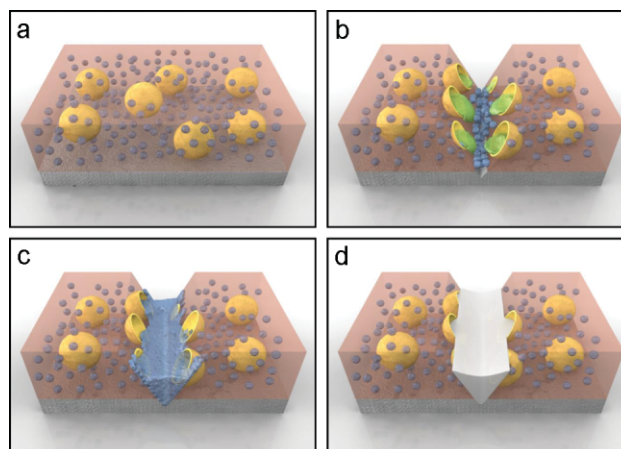


Figure 1. Schematic of self-healing process. a) Self-healing coating containing microencapsulated catalyst (yellow) and phase-separated healing-agent droplets (blue) in a matrix (light orange) on a metallic substrate (grey). b) Damage to the coating layer releases catalyst (green) and healing agent (blue). c) Mixing of healing agent and catalyst in the damaged region. d) Damage healed by cross-linked PDMS, protecting the substrate from the environment.

[*] Prof. P. V. Braun
Beckman Institute
Department of Materials Science and Engineering
and Frederick Seitz Materials Research Laboratory
University of Illinois at Urbana-Champaign
Urbana, IL 61801, USA
E-mail: pbraun@illinois.edu

Dr. S. H. Cho
Beckman Institute
and Department of Materials Science and Engineering
University of Illinois at Urbana-Champaign
Urbana, IL 61801, USA

Prof. S. R. White
Beckman Institute
Department of Materials Science and Engineering
and Department of Aerospace Engineering
University of Illinois at Urbana-Champaign
Urbana, IL 61801, USA

DOI: 10.1002/adma.200802008

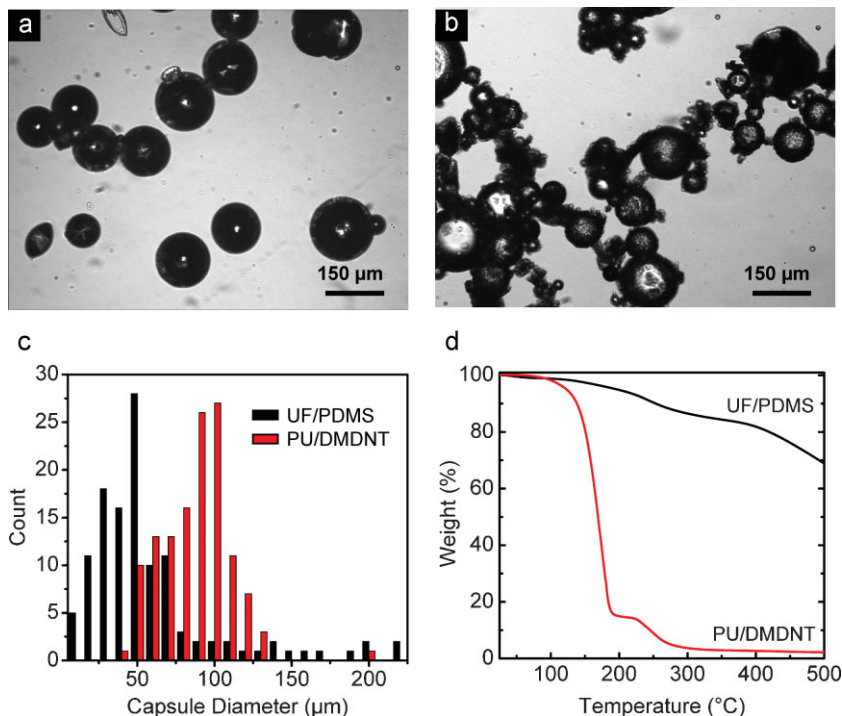


Figure 2. a,b) Optical microscopy images of a) DMDNT-containing PU microcapsules and b) PDMS healing-agent-filled UF microcapsules. c) Size histogram for both microcapsules. d) Thermogravimetric analysis of both microcapsules.

diameter (Fig. 2a and c), and upon thermogravimetric analysis (TGA) exhibit a primary weight loss starting near the boiling point of chlorobenzene (131 °C), and a secondary weight loss starting at 225 °C, corresponding to thermal decomposition of the polyurethane shell (Fig. 2d).

The self-healing function of this coating system is evaluated through corrosion testing of damaged and healed coated steel samples compared to control samples (Fig. 3 and Supporting Information Fig. S1). Damage is induced by hand scribing through the 100 μm thick coating and into the substrate using a razor blade. Because the substrate is significantly harder than the coating, the scribe depth is uniform to within ~10 μm. Following the scribing procedure, samples are allowed to heal at 50 °C for 24 h. Samples are then immersed in 5 wt% aqueous NaCl solution for a prescribed period of time. All control samples rapidly corrode within 24 h, and exhibit extensive rust formation, most prevalently within the groove of the scribed regions, but also extending across the substrate surface. In dramatic contrast, the self-healing samples show no visual evidence of corrosion, even 120 h after exposure (Fig. 3b); these experiments are highly reproducible. Separate control tests reveal that the presence of both the healing agent and catalyst are necessary for self-healing functionality. Removal of either phase results in a coating which corrodes rapidly, providing a clear indication that simple reflow of one of the phases into the crack is not sufficient to prevent corrosion (Supporting Information, Fig. S1). The bifunctional adhesion promoter, which served to enhance the bonding between the silane-based healing agent and the epoxy vinyl ester matrix, is not necessary for self-healing. However, in its absence the cured

PDMS does not always remain in the scratch after healing, leading to corrosion of the underlying substrate.

Scanning electron microscopy (SEM) imaging of the scribe region in control and self-healing coatings reveals the morphology of the repaired coating (Fig. 3c and d). Flow of healing agent and catalyst into the scribe and recoating (passivation) of the substrate is readily apparent. The damage is significantly (~40%) filled by polymerized healing agent in the self-healing coating, while the scribe extends about 15 μm into the metal substrate in the control sample (Supporting Information, Table S1). Profilometry measurements and energy-dispersive spectroscopy of nickel-coated cross-sectioned samples (post-healing) confirmed these findings (Supporting Information, Fig. S2).

Electrochemical testing provides further evidence of passivation of the substrate by self-healing coatings. In these experiments, the coated metal substrate serves as one electrode in an electrochemical cell (Fig. 3e). The steady-state conduction between the coated metal substrate and a platinum electrode held at 3 V through an aqueous electrolyte (1 M NaCl) is measured (Fig. 3f). The current passing through the control and self-healing polymer coatings before scribing are nearly identical, ~0.34 μA cm⁻². After scribing, samples are allowed to heal and are tested in the electrochemical cell. The current passing through the scribed control samples is quite large (26.6–58.6 mA cm⁻², three samples), compared to the undamaged state, and we note rapid gas evolution from the scribed region during the test. The self-healing samples show a dramatically reduced current (12.9 μA cm⁻²–1.4 mA cm⁻², four samples), and no gas evolution is observed from the self-healing sample.

While this model coating system consisting of phase-separated PDMS healing agents and microencapsulated catalyst has impressive properties, some limitations are apparent. First, the PDMS healing agents are in direct contact with the coating matrix, and are thus susceptible to matrix-initiated reactions. For example, amine curing agents found in many epoxies catalyze PDMS healing-agent condensation. To overcome this limitation, and provide a more general approach, the PDMS healing agent phase is encapsulated within urea-formaldehyde (UF) microcapsules, to produce a dual capsule self-healing coating system, comprised of 12 wt% PDMS-filled UF microcapsules, 3 wt% DMDNT catalyst-filled PU microcapsules, and 3 wt% adhesion promoter dispersed in an epoxy-amine matrix. In this case, the healing agent is now protected by the UF shell wall from direct contact with the matrix polymer. The PDMS healing-agent capsules averaged 60 μm in diameter (Fig. 2b and c). TGA of these capsules shows a slow weight loss beginning at 150 °C (Fig. 2d); the overall small weight loss of these capsules at even 500 °C is due to the high thermal stability of PDMS. In preliminary corrosion testing of this epoxy-based coating,

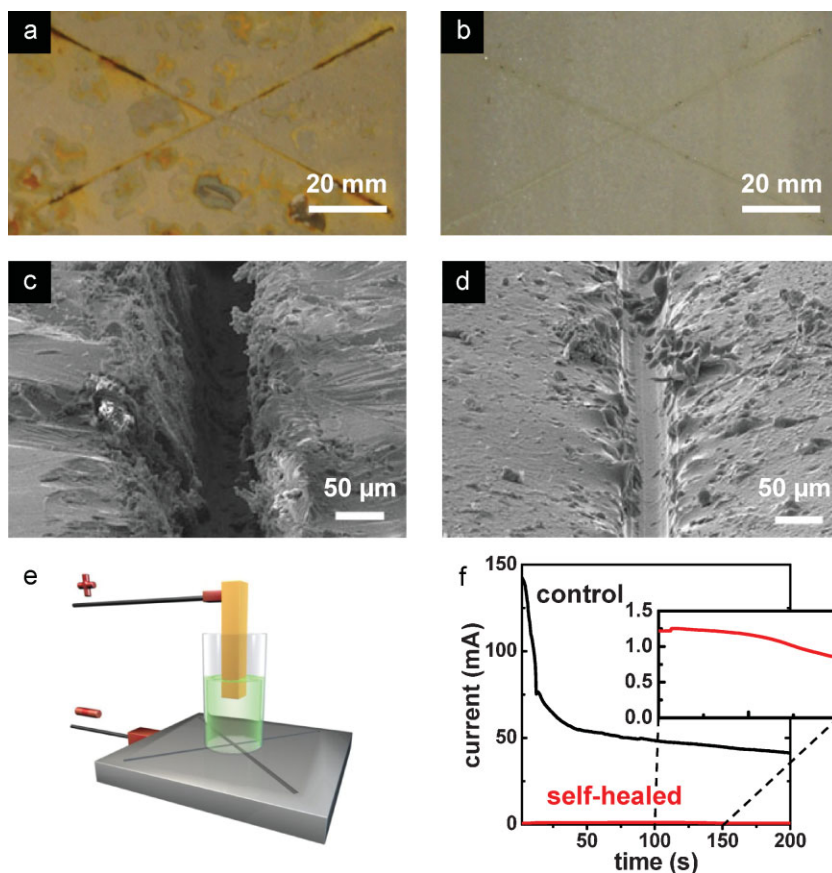


Figure 3. Corrosion, morphological, and electrochemical evaluation of self-healing coatings. a,b) Optical images after 120 h immersion in salt water of a) control sample, consisting of the epoxy vinyl ester matrix and adhesion promoter, and b) self-healing coating, consisting of matrix, adhesion promoter, microencapsulated catalyst, and phase-separated PDMS healing agent. c,d) SEM images of the scribed region of the control coating c) and the self-healing coating after healing d). e) Schematic diagram of electrochemical test. f) Current versus time for scribed control and self-healed sample.

adhesion to the substrate was found to be inadequate, and thus a 50 μm thick epoxy-based primer layer is applied to the substrate, and cured prior to coating application. Corrosion-test results for 100 μm thick control and dual capsule self-healing coating samples are virtually identical to our observations on the phase-separated system (Fig. 3). All control samples show extensive corrosion following 120 h of salt water exposure, while self-healed samples (healed for 24 h at 50 $^{\circ}\text{C}$) show no evidence of rust formation (Supporting Information, Fig. S3)

True self-healing requires no external intervention, including heating to temperatures greater than ambient, a requirement we note for our model coating system using DMDNT as the catalyst phase. This catalyst has reduced activity at room temperature, and although corrosion tests demonstrated some level of self-healing at room temperature, healing performance for this system is not ideal. Room temperature ($\sim 20^{\circ}\text{C}$) self-healing is achieved through the synthesis and encapsulation of $\text{Si}[\text{OSn}(\text{n-C}_4\text{H}_9)_2\text{OOCCH}_3]_4$, (TKAS), a highly effective catalyst for curing PDMS. The diameter and morphology (Supporting Information, Fig. S4) of these capsules is very similar to those of DMDNT-filled capsules presented in Figure 2. Along with

room-temperature activity, unlike DMDNT this catalyst does not require moisture for activation,^[25–27] potentially enabling self-healing coatings for moisture-free environments, such as found in aerospace applications or at buried interfaces. The corrosion performance of the dual-capsule room-temperature system is demonstrated by the incorporation of self-healing components into both a general epoxy-based coating system and a commercial marine (epoxy) coating system (Fig. 4). For both systems, 3 wt% TKAS catalyst-filled PU microcapsules, 14 wt% PDMS healing-agent-containing UF capsules, and 3 wt% adhesion promoter are added to the appropriate matrix. A coating 100 μm thick is placed onto the primed steel substrate and cured. For the marine coating, a second layer 100 μm thick (without self-healing components) is applied, to provide a smooth surface texture. Corrosion-test results after scribing and healing for 24 h at room temperature show the efficacy of the room-temperature activity for both these systems (Fig. 4).

Our dual-capsule PDMS healing system provides a general approach to self-healing coatings that place rigorous demands on chemical compatibility and stability. By incorporating TKAS catalyst, we show that autonomic corrosion protection can be obtained by self-healing under ambient environmental conditions. Multilayered coatings can also be formulated to provide self-healing functionality while maintaining extreme tolerances on surface finish, specific requirements for engineered primers, or unique surface chemistries (e.g., self-cleaning). We believe the microcapsule motif also provides a delivery mechanism for multifunctional chemical agents, which provide healing as well as corrosion inhibitors,^[28] antimicrobial agents,^[29] or other functional chemicals.

Experimental

Microcapsules containing 5% DMDNT (Gelest) in chlorobenzene, and 2% TKAS in chlorobenzene, were microencapsulated within polyurethane capsules, as previously described [21]. PDMS healing-agent-filled urea-formaldehyde microcapsules were formed following our published procedure [1] with the following modifications. 250 mL of reaction mixture was heated to 55 $^{\circ}\text{C}$ and stirred at 700 rpm. 60 mL of a mixture of the PDMS healing agent, HOPDMS (48 mL), PDES (2 mL), and n-heptane (10 mL) was added. After 4 h, the reaction mixture was cooled to room temperature, and the microcapsules were separated.

TKAS, $\text{Si}[\text{OSn}(\text{n-C}_4\text{H}_9)_2\text{OOCCH}_3]_4$, was synthesized following US patent 4,137,249 [27]. 0.1 mol of di-n-butyltin diacetate and 0.025 mol of tetraethylsilicate were first mixed in a round flask. The solution was heated to 150 $^{\circ}\text{C}$ while stirring under anhydrous conditions. The reaction by-product, ethyl acetate, was distilled off at atmospheric pressure. The ethyl acetate started to condense at 130 $^{\circ}\text{C}$, and most of it was removed after 15 min at 150 $^{\circ}\text{C}$. The crude TKAS reaction product has the form of

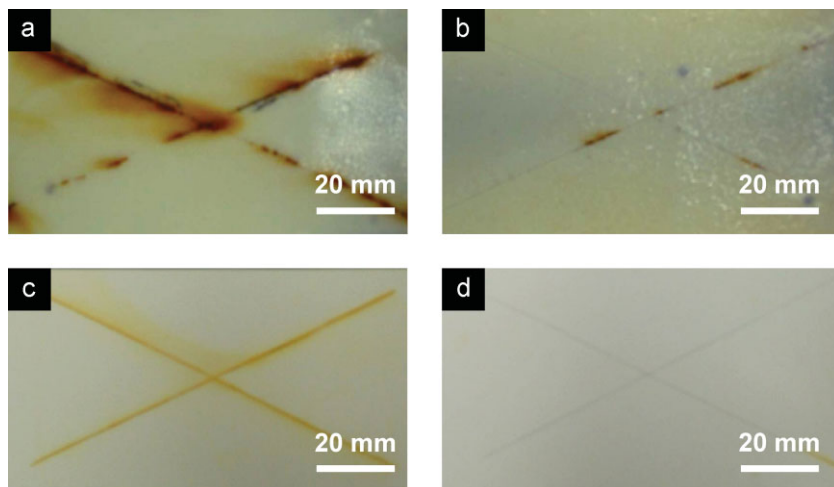


Figure 4. Salt-immersion corrosion testing of control and of room-temperature self-healing epoxy coatings. All images were obtained after heating at 20 °C for 24 h and 120 h immersion in salt water. a) Control coating, consisting of the epoxy-amine matrix containing adhesion promoter coated on a primed substrate. b) The self-healing coating prepared as a), with the addition of PDMS healing-agent capsules and TKAS-catalyst capsules. c) Two-layer commercial marine coating, containing adhesion promoter (control sample). d) Self-healing coating prepared as c), with the addition of PDMS healing-agent capsules and TKAS-catalyst capsules.

wax-like spherulites, which dissolve in chlorobenzene. The reaction product was further purified by recrystallization. 1 g of crude TKAS was dissolved in 10 mL of chlorobenzene at 80 °C. The solution was cooled with an ice bath, and the purified TKAS was harvested by filtration.

All coatings were applied to 75 mm × 150 mm cold-rolled steel sheets, using a micrometer-controlled doctor blade. Coating solutions were applied to one end of the substrate, and the doctor blade was used to spread a uniform-thickness coating.

The self-healing epoxy vinyl ester coating was formed by dissolving 1 wt% benzoyl peroxide (polymerization initiator) in the vinyl ester prepolymer (Ashland, Derakane 510A-40). After the benzoyl peroxide was completely dissolved, 12 wt% PDMS healing agent, a mixture of 96 vol% HOPDMS and 4 vol% PDES (Gelest), and 3 wt% adhesion promoter, methylacryloxy propyl triethoxy silane (Gelest), was added into the prepolymer with mechanical stirring, followed by degassing under vacuum. Then, 3 wt% microcapsules containing DMDNT catalyst were mixed with the degassed solution, and 0.1 wt% dimethylaniline (activator) was added, followed by a final degassing. Samples were coated on the substrate with a thickness of 100 μm, and cured at room temperature for 24 h prior to testing.

The epoxy-amine self-healing coating is composed of epoxy (Epon[®] 828) mixed with 12 wt% diethylenetriamine, 3 wt% adhesion promoter, (3-trimethoxysilylpropyl) dimethylene triamine (Gelest), 3 wt% DMDNT- or TKAS catalyst-containing microcapsules, and 14 wt% of PDMS-containing microcapsules. The coating solution was mixed by mechanical stirring, followed by degassing under vacuum. A layer 50 μm thick of a commercial epoxy-based primer (Kukdo Chemical, KU-420K40) was first coated on the metal substrate. After the primer cures, 100 μm of the epoxy-amine system was coated on the primer layer. Samples were then cured at room temperature for 24 h and 30 °C for 24 h, prior to testing.

The self-healing commercial marine (epoxy) coating was formed by mixing International Marine Coatings, Intergard 264, with 3 wt% adhesion promoter, (3-trimethoxysilylpropyl) dimethylene triamine, 3 wt% of TKAS-containing microcapsules, and 14 wt% of PDMS-containing microcapsules. Samples were coated on the substrate with a thickness of 100 μm, and cured at room temperature for 24 h and 30 °C for 24 h.

A 100 μm layer of Intergard 264 was subsequently applied over the self-healing layer, and similarly cured.

Acknowledgements

This work has been principally sponsored by Northrop Grumman Ship Systems (SRA 04-307), as well as the Air Force Office of Scientific Research and by the Beckman Institute for Advanced Science and Technology at the University of Illinois at Urbana-Champaign. The authors gratefully acknowledge A. Jackson for assistance with TGA and optical microscopy, and helpful discussions with Prof. N. Sottos, Prof. J. Moore, X. Yu, and R. Shimmin. Supporting Information is available online from Wiley InterScience or from the author.

Received: July 15, 2008

Revised: October 17, 2008

Published online: December 2, 2008

- [1] S. R. White, N. R. Sottos, P. H. Geubelle, J. S. Moore, M. R. Kessler, S. R. Sriram, E. N. Brown, S. Viswanathan, *Nature* **2001**, 409, 794.
- [2] E. N. Brown, S. R. White, N. R. Sottos, *J. Mater. Sci.* **2004**, 39, 1703.
- [3] J. D. Rule, E. N. Brown, N. R. Sottos, S. R. White, J. S. Moore, *Adv. Mater.* **2005**, 17, 205.
- [4] M. W. Keller, S. R. White, N. R. Sottos, *Adv. Funct. Mater.* **2007**, 17, 2399.
- [5] M. M. Caruso, D. A. Delafuente, V. Ho, N. R. Sottos, J. S. Moore, S. R. White, *Macromolecules* **2007**, 40, 8830.
- [6] T. Yin, M. Z. Rong, M. Q. Zhang, G. C. Yang, *Compos. Sci. Technol.* **2007**, 67, 201.
- [7] D. G. Shchukin, H. Mohwald, *Small* **2007**, 3, 926.
- [8] X. X. Chen, M. A. Dam, K. Ono, A. Mal, H. B. Shen, S. R. Nutt, K. Sheran, F. Wudl, *Science* **2002**, 295, 1698.
- [9] X. X. Chen, F. Wudl, A. K. Mal, H. B. Shen, S. R. Nutt, *Macromolecules* **2003**, 36, 1802.
- [10] F. R. Kersey, D. M. Loveless, S. L. Craig, *J. R. Soc. Interface* **2007**, 4, 373.
- [11] P. Cordier, F. Tournilhac, C. Soulie-Ziakovic, L. Leibler, *Nature* **2008**, 451, 977.
- [12] K. S. Toohey, N. R. Sottos, J. A. Lewis, J. S. Moore, S. R. White, *Nat. Mater.* **2007**, 6, 581.
- [13] J. Y. Lee, G. A. Buxton, A. C. Balazs, *J. Chem. Phys.* **2004**, 121, 5531.
- [14] S. Gupta, Q. L. Zhang, T. Emrick, A. C. Balazs, T. P. Russell, *Nat. Mater.* **2006**, 5, 229.
- [15] R. Verberg, A. T. Dale, P. Kumar, A. Alexeev, A. C. Balazs, *J. R. Soc. Interface* **2007**, 4, 349.
- [16] C. S. Coughlin, A. A. Martinelli, R. F. Boswell, *PMSE Preprints* **2004**, 91, 472.
- [17] S. J. Kalista, T. C. Ward, *J. R. Soc. Interface* **2007**, 4, 405.
- [18] D. V. Andreeva, D. Fix, H. Mohwald, D. G. Shchukin, *Adv. Mater.* **2008**, 20, 1.
- [19] J. W. C. Pang, I. P. Bond, *Compos. Sci. Technol.* **2005**, 65, 1791.
- [20] J. W. C. Pang, I. P. Bond, *Composites Part A* **2005**, 36, 183.
- [21] S. H. Cho, H. M. Andersson, S. R. White, N. R. Sottos, P. V. Braun, *Adv. Mater.* **2006**, 18, 997.
- [22] G. H. Koch, M. P. Brongers, N. G. Thompson, Y. P. Virmani, J. H. Payer, *Corrosion Costs and Preventive Strategies in the United States*,

- FHWA-RD-01-156, U. S. Department of Transportation, Federal Highway Administration, Washington D.C., **2001**.
- [23] A. S. Jones, J. D. Rule, J. S. Moore, N. R. Sottos, S. R. White, *J. R. Soc. Interface* **2007**, *4*, 395.
- [24] M. W. Keller, S. R. White, N. R. Sottos, *Polymer* **2008**, *49*, 3136.
- [25] G. B. Shah, *J. Appl. Polym. Sci.* **1998**, *70*, 2235.
- [26] F. W. Van der Weij, *Macromol. Chem.* **1980**, *181*, 2541.
- [27] E. Wohlfarth, W. Hechtel, P. Hittmair, *US Patent* 4,137,249, **1979**.
- [28] V. S. Sastri, *Corrosion Inhibitors: Principles and Applications*, Wiley, New York **1998**.
- [29] A. Bryskier, *Antimicrobial Agents: Antibacterials and Antifungals*, ASM Press, Washington **2005**.
-